doi: 10.13133/2280-6148/17274 *Journal of Mediterranean Earth Sciences 13 (2021), 19-30*

J M E S **Journal of Mediterranean Earth Sciences**

U-Pb SIMS zircon ages for Cambro-Ordovician rocks, Valongo Anticline, northwestern Portugal

Michael E. Brookfield [1,*], Helena Couto [2], Elizabeth J. Catlos [1], Axel Schmitt [3]

[1] *Department of Geological Sciences, Jackson School of Geosciences, The University of Texas at Austin, Austin, Texas, USA*
[2] *Department of Geosciences, Environment and Spatial Planning, ICT- Institute of Earth Sciences, University of Porto, Faculty of Sciences, Portugal*
[3] *Institut für Geowissenschaften, Universität Heidelberg, Im Neuenheimer Feld 234-236 69120 Heidelberg, Germany*
**Corresponding author: mbrookfi@hotmail.com*

ABSTRACT - The development of the NW Gondwanan Lower Paleozoic passive margin requires accurate dating of its Cambro-Ordovician rocks. In northern Portugal, major bimodal volcanism associated with rifting during the Cambrian to earliest Ordovician is poorly constrained biostratigraphically. To contribute to resolving the ages of these rocks, we dated zircons from samples from the continental rift valley to subsiding passive margin succession in the Valongo Anticline of NW Portugal with U-Pb secondary ion mass spectrometry (SIMS). Only three samples analyzed contained zircons. A rhyolite near the top of the supposed Cambrian Montalto Formation gave clusters of Lower Paleozoic (609 to 454 Ma) and Upper Carboniferous zircon ages (332 to 297 Ma), with one Paleoproterozoic age (1743 Ma). The youngest concordant age of 516±16 Ma ($^{238}U/^{206}Pb$, ±1σ) of this rhyolite may be the best age for the top of the Montalto Formation, which puts it as equivalent to Middle Cambrian Series 2. The youngest Upper Carboniferous age clusters (332 to 297 Ma) are caused by zircon alteration or hydrothermal recrystallization during the Variscan orogeny. A black chert sample, underlying the massive supposed Arenigian quartzites of the Santa Justa Formation, gave two detrital zircon ages of 827±36 Ma and 492±12 Ma, the latter indicating a maximum latest Cambrian (Furongian) age. A volcanic sandstone, overlying these quartzites gave mostly Neoproterozoic detrital zircon ages (933±44 to 560±15 Ma), which may derive from erosion of regional basement of the Sahara metacraton far to the southeast. Our results, though limited in number, indicate that only the upper quartzite part of the Santa Justa Formation could be equivalent to the so-called Arenigian quartzites (also poorly constrained) in NW France and Iberia. The Upper Cambrian seems to be missing in the studied area where a major unconformity probably occurs below the lower Santa Justa Formation.

Keywords: U/Pb; geochronology; Cambrian-Ordovician; Valongo; anticline; Portugal.

Submitted: 26 December 2020-Accepted: 2 August 2021

1. INTRODUCTION

Early Paleozoic rocks of Iberia outcrop in several distinct tectonic units deformed and assembled during the late Paleozoic Variscan orogeny and further rotated anticlockwise during the opening of the Atlantic Ocean (Ribeiro et al., 2007; Stampfli and Borel, 2002) (Fig. 1A). Most of the Iberian tectonic zones are originally from Gondwanaland, with the exception of the allochthonous South Portuguese Zone which is separated from the Ossa Morena Zone by an ophiolitic suture (Fig. 1B). The other Iberian zones, the Ossa Morena, Lusitanian-Alcidian, Galician-Castilian and Asturian-Leonese Zones are all Gondwana-derived. Though separated by major transcurrent faults, no oceanic sutures exist between them, and their Ordovician stratigraphies are sufficiently alike to suggest that these faults are not plate boundaries (Lotze, 1945; Romano, 1982; Gutiérrez-Marco et al., 2015). The Valongo Anticline is located in the northern Lusitanian Zone, which is separated by major strike-slip faults from Galician-Castilian Zone on the northeast (both combined as the Central Iberian Zone to the southeast) and the Ossa-Moreno Zone to the southwest (Romano, 1982). Further southwest, an ophiolitic suture separates the allochthonous South Portuguese Zone from the Ossa Morena Zone, and the Central Iberian Zone is thrust northeast over the Asturian-Leonese Zone of the Variscan foreland with its thick Gondwana-related

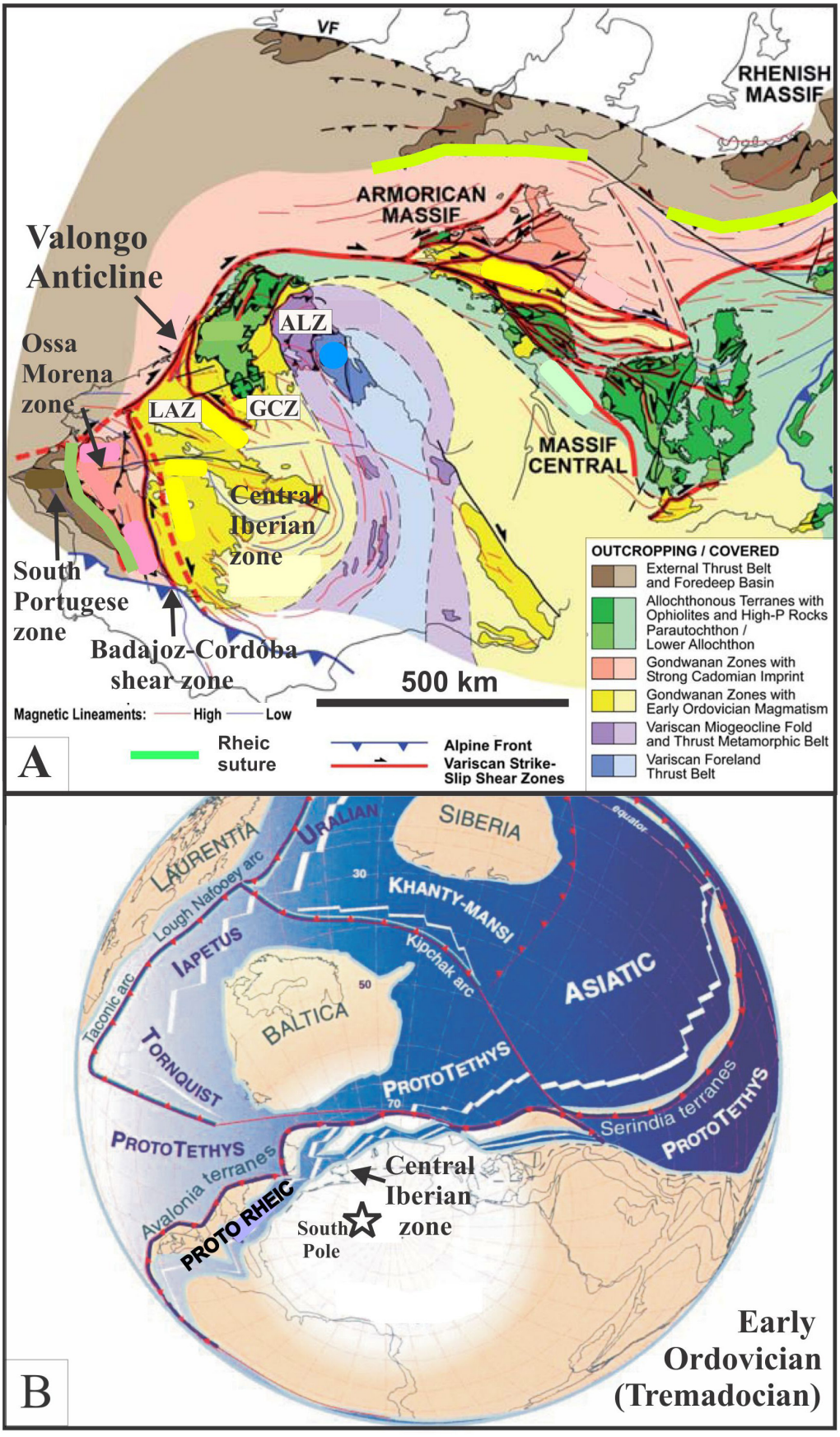

Fig. 1 - A) Tectonostratigraphic map of the Western European Variscan belt (after Catalán, 2011) showing position of Valongo anticline. LAZ - Luso-Alcidian subzone, GCZ - Galician-Castilian Zone, ALZ - Asturias-Leonese Zone; B) Early Ordovician southern hemisphere paleogeography (after Stampfli and Borel, 2002).

Cambro-Ordovician clastics (Catalán, 2011) (Fig. 1A).

The original position of these units in the early Paleozoic is debatable, partly due to lack of appreciation of the importance and effects of major tectonic structures, such as thrusts, strike-slip shear zones, and oroclines (Catalán, 2011). A reasonably objective original position for the Central Iberian zone is on the north-facing Gondwana shelf during its rifting to begin forming the Rheic Ocean, at very high latitudes, close to the South Pole (Murphy et al., 2006; Linnemann et al., 2008) (Fig. 1B).

The supposed Upper Cambrian to Lower Ordovician succession of the Central Iberian Zone consists dominantly of clastic metasediments, locally interbedded with magmatic subvolcanic and volcanic rocks and is very poorly dated as it mainly consists of coarse shallow marine to continental sediments and lavas without diagnostic fossils (Couto,1993, Couto and Roger, 2017). The succession is underlain by Middle Cambrian clastics (Liñán et al., 1993) and passes up into Oretanian stage (roughly equal to British Llanvirn and International Darriwilian stages) fine-grained clastics (Reyes-Abril et al., 2010). The Upper Cambrian to Lower Ordovician ages assigned to of these units is therefore primarily based on stratigraphic position.

In order to determine the ages of these sediments, we obtained reconnaissance U-Pb Secondary Ion Mass Spectrometry (SIMS) zircon ages from three layers in the Valongo Anticline. The ages reported here, though somewhat inconclusive due to the limited number of crystals available for analysis, not only suggest predominantly late Pre Cambrian ages for the source rocks of the anatectic rhyolites but indicate that sediment sources are similar to those from higher-grade metasediments of the North Gondwana block in the Pyrenees (Margalef et al., 2016). They are the first radiometric dates from this succession in the Valongo Anticline.

2. GEOLOGICAL SETTING AND ANALYZED SAMPLES

The Valongo Anticline is located in Northern Portugal, in the Central-Iberian Zone (Fig. 2). It is a major pre-Stephanian asymmetrical antiform trending southeast, with an axial plunge towards the northwest and surrounded by Variscan granites (Ribeiro et al., 2007). The Paleozoic stratigraphic succession consists of folded Cambrian to Devonian volcanic rocks and clastic sediments, overlain by Carboniferous age continental sediments west of the inverse limb of the Valongo Anticline (Fig. 2). Sb-Au mineralization of the Valongo anticline and Douro Shear Zone (Couto, 1993; Couto and Roger, 2017), part of the extensive Sb-Au Variscan mineralization of Armorica (Pochon et al., 2018).

2.1. THE CAMBRO-ORDOVICIAN SUCCESSION

The Montalto Formation consists of continental

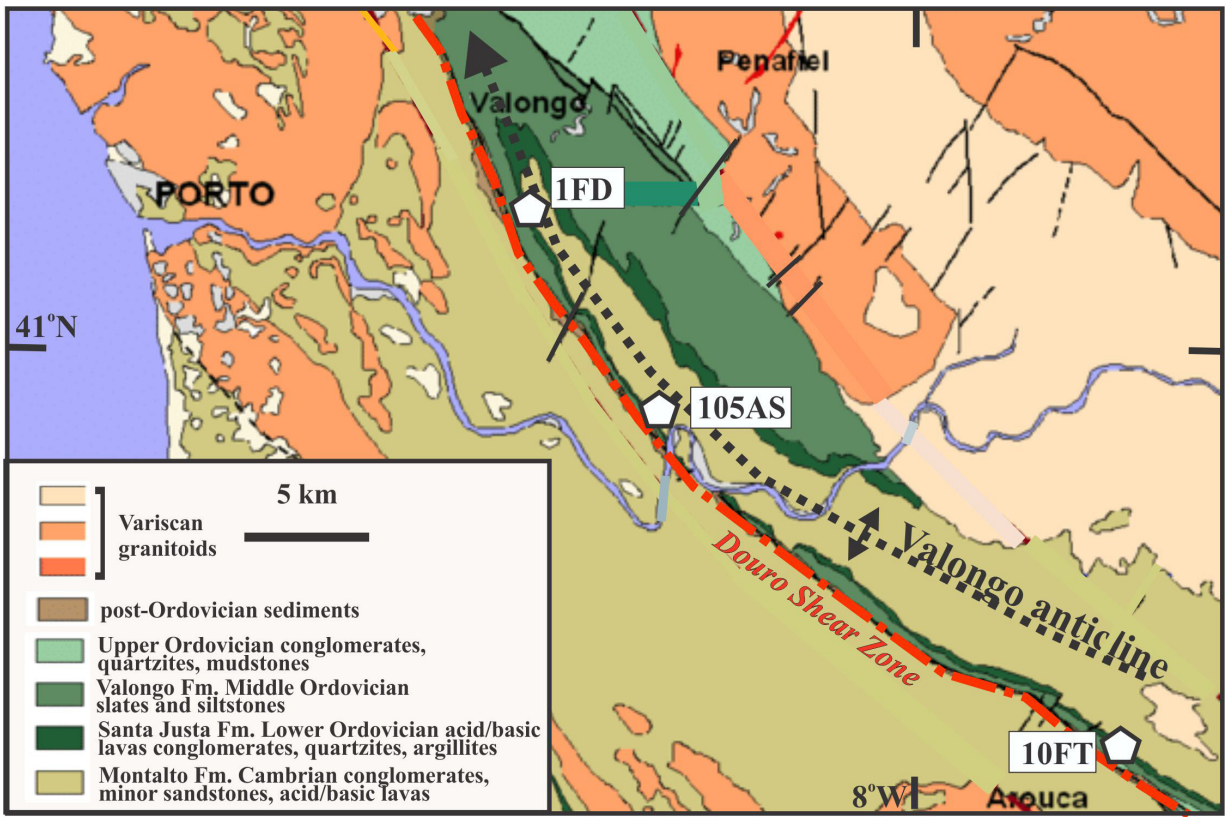

Fig. 2 - Geological map of Valongo Anticline showing location of analyzed samples: 10FT - Fragas daTorre; 1FD - Fragas do Diabo; and 105AS - Alto do Sobrido, Gondomar (after Gonçalves, 2013).

clast-supported conglomerates with minor argillites and quartzites and quartz greywacke intercalations interbedded with bimodal rhyolite- basalt lavas (Couto and Knight, 2014). The lowermost conglomerates have quartzite pebbles, while the topmost ones have more varied pebbles of quartz, schist, and black quartzite (Couto, 2013). The clastics are typical continental braided stream facies and are unfossiliferous, so their Upper Cambrian attribution is tentative (Couto, 2013). Together with the bimodal lavas they are a typical continental rift assemblage.

The Santa Justa Formation rests unconformably on the Montalto Formation. It is a seemingly continuous 60-metre-thick succession of typically rapidly deposited sediments and lavas unbroken by unconformities, with the transgressive Valongo Formation conformably above (Fig. 3). A lower continental unit consists of coarse clastic sediments interbedded with bimodal basalt-rhyolite lavas, like the Montalto Formation (Couto, 2013). A marginal marine middle unit is dominated by quartzites, which contain *Cruziana* trace fossils of probably Arenigian age (Romano and Diggens, 1974; Sá et al., 2011). An upper unit consists of probably marginal marine volcaniclastic sandstones with oolitic ironstones at their base (Couto, 1993; Couto and Moëlo, 2011). These ironstones form distinctive Ordovician facies on the northwestern Gondwana platform and its dispersed fragments, in Newfoundland, Wales, western Europe and northwestern Africa (Young, 1992). Towards the top of the Santa Justa Formation, a phosphate-rich lingulid shell bed marks the

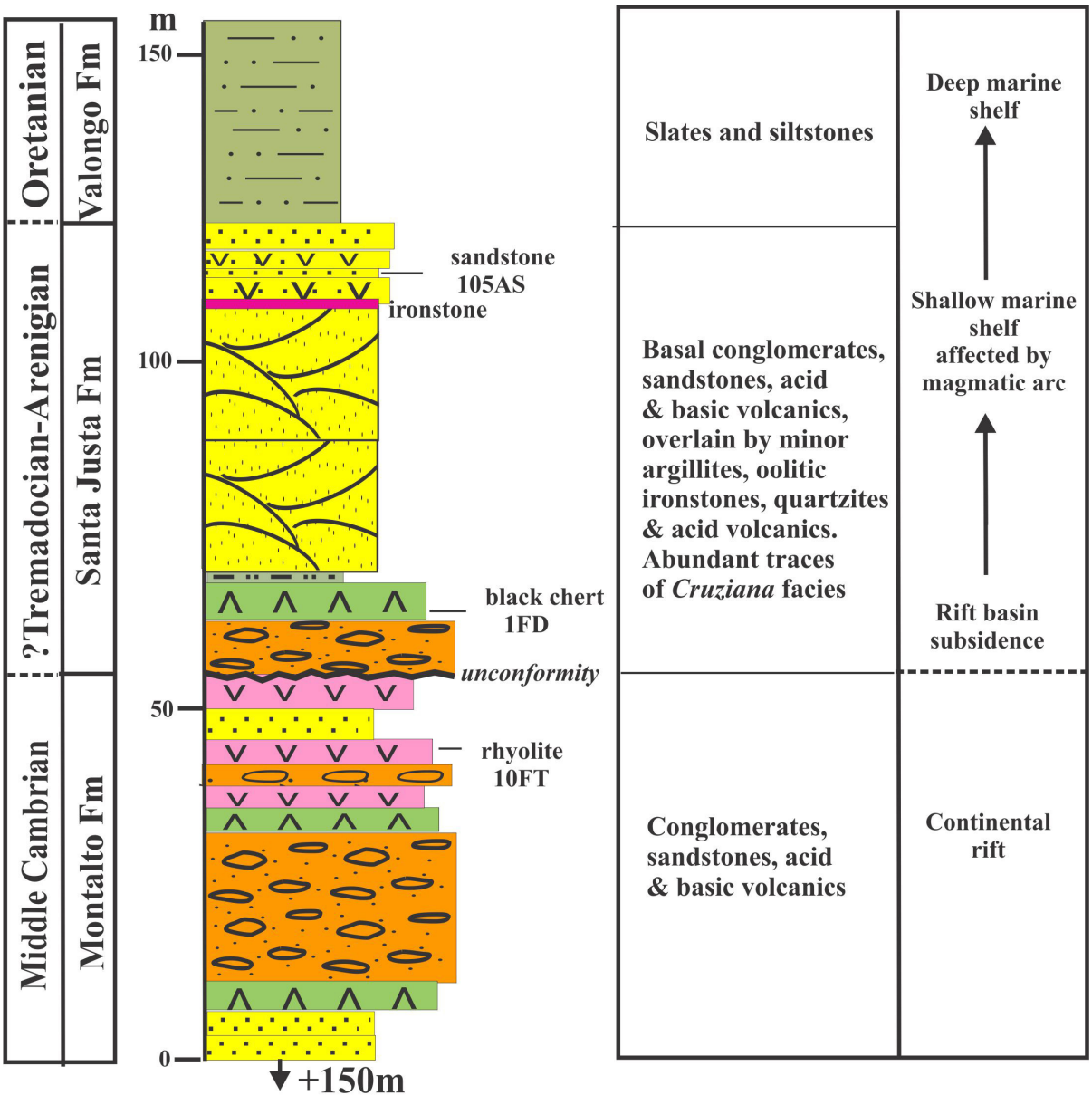

Fig. 3 - Cambrian to Ordovician stratigraphic column of Valongo Anticline with inferred paleoenvironments and dated samples (from Couto and Roger, 2017).

transgressive transition to the Valongo Formation.

The Valongo Formation consists of marine shales and siltstones, and is renowned for its diverse fauna, including giant trilobites (Gutiérrez-Marco et al., 2009). Near its base the fossils indicate an Oretanian age, roughly equivalent to the lower Llanvirn Series and Middle Darriwilian stage (Couto, 1993; Gutiérrez-Marco et al., 2015, 2017).

The Santa Justa and Valongo Formations form a typical continental rifting to subsiding passive margin assemblage, with the post-rifting unconformity at the base of the Santa Justa Formation, and, like the Mesozoic to Cenozoic Atlantic margin, is unlikely to have any major time gaps (Soares et al., 2012; Mohriak and Leroy, 2013).

2.2. SAMPLES ANALYZED

Our samples come from the inverted limb of the Valongo Anticline whose succession is tectonically thinned and the stratal thicknesses shown in figure 3 may be too thin in consequence (Romano and Diggens, 1974), Of the samples collected, only three from the Montalto and Santa Justa Formations had suitable zircons for analysis (Fig. 3) (Couto and Roger, 2017). Sample 10FT is from a rhyolite lava near the top of the Montalto Formation at Fragas da Torre (Arouca) and has quartz and alkali feldspar phenocrystals in a fine-grained groundmass. Quartz phenocrysts are both angular and corroded (Fig. 4A). The other two samples are from the Santa Justa Formation. Sample 1FD is from a black chert interbedded with basic volcanics at Fragas do Diabo (Valongo). Sample 105AS is from interbedded thin sandstone and felsic tuffs laminae at Alto do Sobrido (Gondomar) near the top of the Santa Justa Formation. It has rounded quartz and abundant heavy minerals and tuff layers with angular quartz, small sericite skeins resulting from the alteration of feldspars (Fig. 4 B,C). Electron microprobe analysis shows the growth of xenotime on some zircon crystals related to hydrothermal or diagenetic processes, but none of our analyzed zircons had these (Couto et al., 2017).

3. U/PB ZIRCON AGES

3.1. ANALYTICAL TECHNIQUES

Zircons were extracted from each sample by sonicating the crushed samples in a bath of hydrogen peroxide and water, where clay minerals rise to the top of the bath, while zircons and other heavy minerals sink (Hoke et al., 2014). Separated zircons were then analyzed at Heidelberg University (Germany) using the methods of Lukács et al. (2018). Each zircon was examined optically, to eliminate visibly cracked or metamict zircons, mounted in epoxy with AS3 zircon age references (1099.1±0.5 Ma, Schmitz et al., 2003), polished to expose cross sections, and then imaged in cathodoluminescence (CL) (Figs. 5,6). These images were used to determine ideal locations for analysis. Mounts were coated in gold prior to SIMS analysis.

The ages were obtained using a CAMECA ims 1280HR ion microprobe at Heidelberg University (Lukács et al., 2018). In this approach, a mass-filtered ^{16}O- beam (~20 µm diameter spot size) sputters material from the surface to a depth of <5 µm of the zircon grains, and isotopes of U, Th and Pb are detected in a large-radius magnitude spectrometer. Given the small amount of sample consumed, the approach is minimally destructive and allows for future analysis of these grains. During analysis, reflected light images were taken of each spot to determine the spot positions relative to CL zoning of the zircon grains (Figs. 5,6). All standard ages were reduced using a ^{204}Pb common Pb correction, whereas the unknown grains were subjected to both ^{204}Pb and ^{206}Pb corrections (Tab. 1). Isoplot was used to create Concordia plots (Ludwig, 2012) (Fig. 7). The crystallization ages are interpreted from data within ±5% discordance using the $^{238}U/^{206}Pb/^{235}U/^{207}Pb$ age calculation (Tab. 1). All ages plotted on figure 7 are $^{238}U/^{206}Pb$ ages, with ±1σ uncertainty.

4. RESULTS AND INTERPRETATION

Zircon age results are shown on table 1 and Concordia

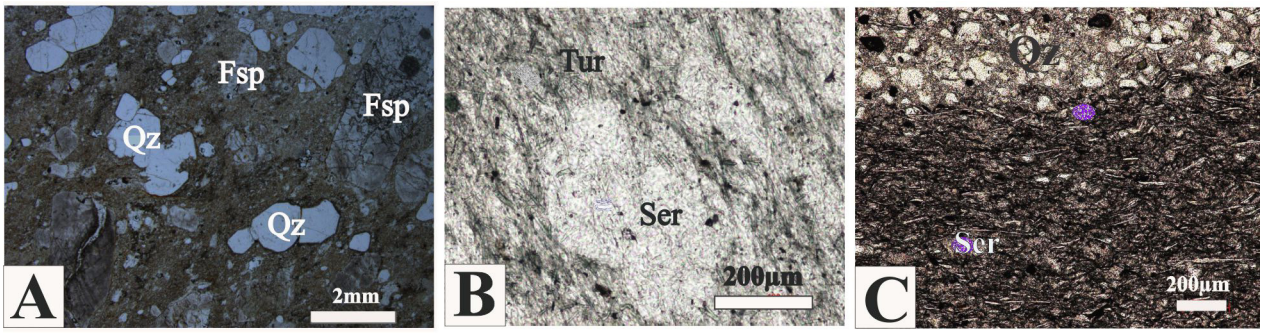

Fig. 4 - Photomicrographs of dated samples in transmitted light. A: Sample 10FT, rhyolite, Fragas da Torre, Arouca; phenocrysts of feldspar (Fsp) and embayed quartz (Qz) in a fine-grained matrix; B: Sample 1FD, black chert, Fragas do Diabo, Valongo; sericite (Ser) in balls (pseudomorphosis after feldspar crystals), opaque minerals and abundant recrystallized tourmaline (Tur); C: Sample 105AS, sandstones interbedded with felsic tuff, Alto do Sobrido, Gondomar; angular quartz crystals (Qz) and flakes of sericite (Ser) resulting from feldspar alteration. Mineral abbreviations from Whitney and Evans (2010).

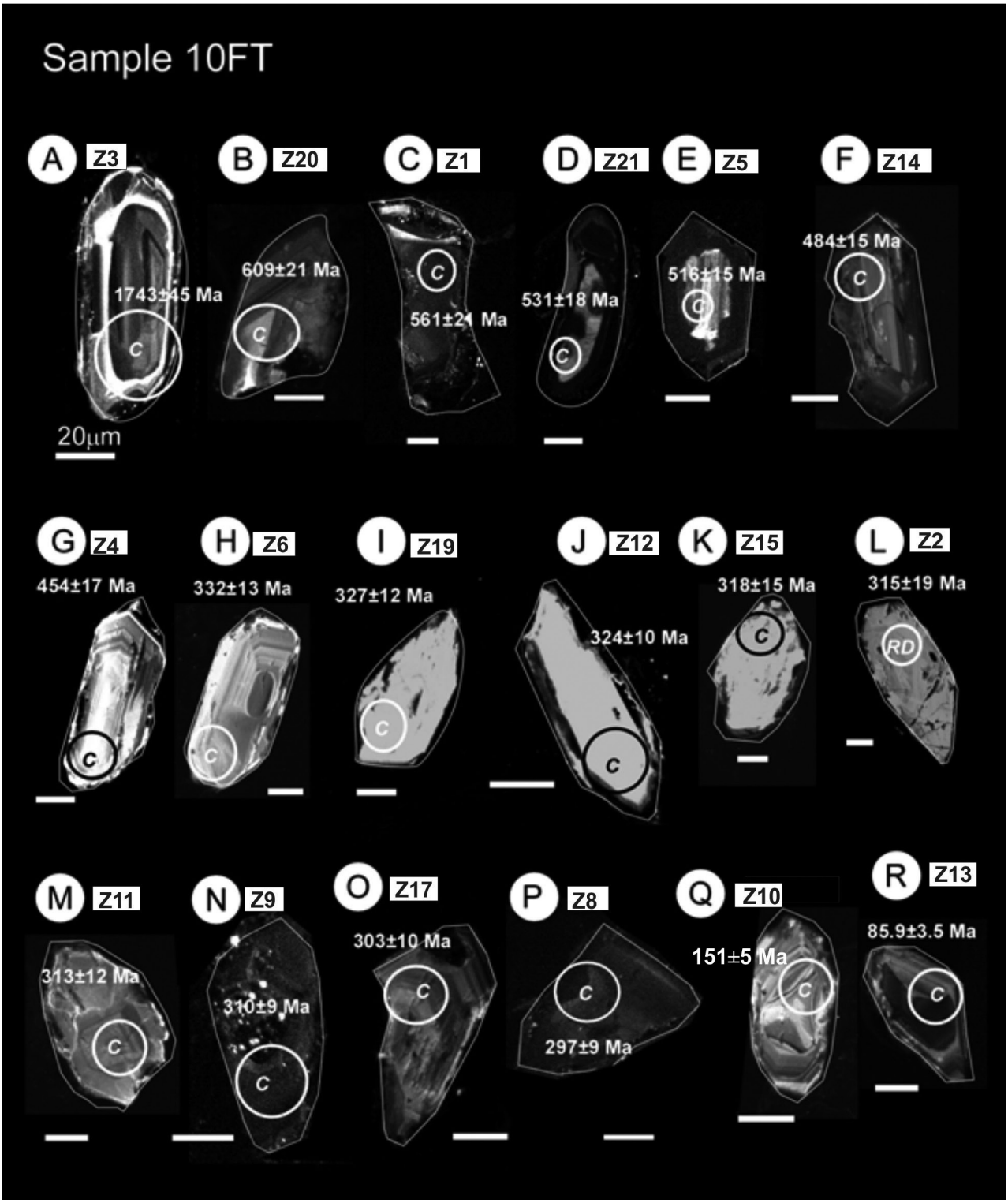

Fig. 5 - CL images of zircons in sample 10FT. C= concordant; D= discordant, and R= reversely discordant. Scale bar is 100μm. Letters for individual zircons on table 1.

plots and age distributions in figure 7. Many zircons have primary oscillatory zoning preserved and these are all concordant (Figs. 5,6). Some zircons are clearly metamorphic in origin with mottled zoning or with textures that suggest alteration (e.g., Fig. 6 E,L). Two zircons clearly show the effects of radiogenic Pb loss with discordant ages (Tab. 1; sample 1FD, Z1; sample 105AS, Z6a) (Fig. 6 L,D). Others are near-concordant but give anomalously young apparent $^{206}Pb/^{238}U$ ages; those younger than about 350 Ma (Fig. 5 H-L). Two are very much younger and may reflect hydrothermal alteration during post-Variscan faulting and mineralization (Z10, Z13; Fig. 5 Q,R). Several show reverse discordances (sample 10FT, Z14 and Z4; sample 1FD, Z2; sample

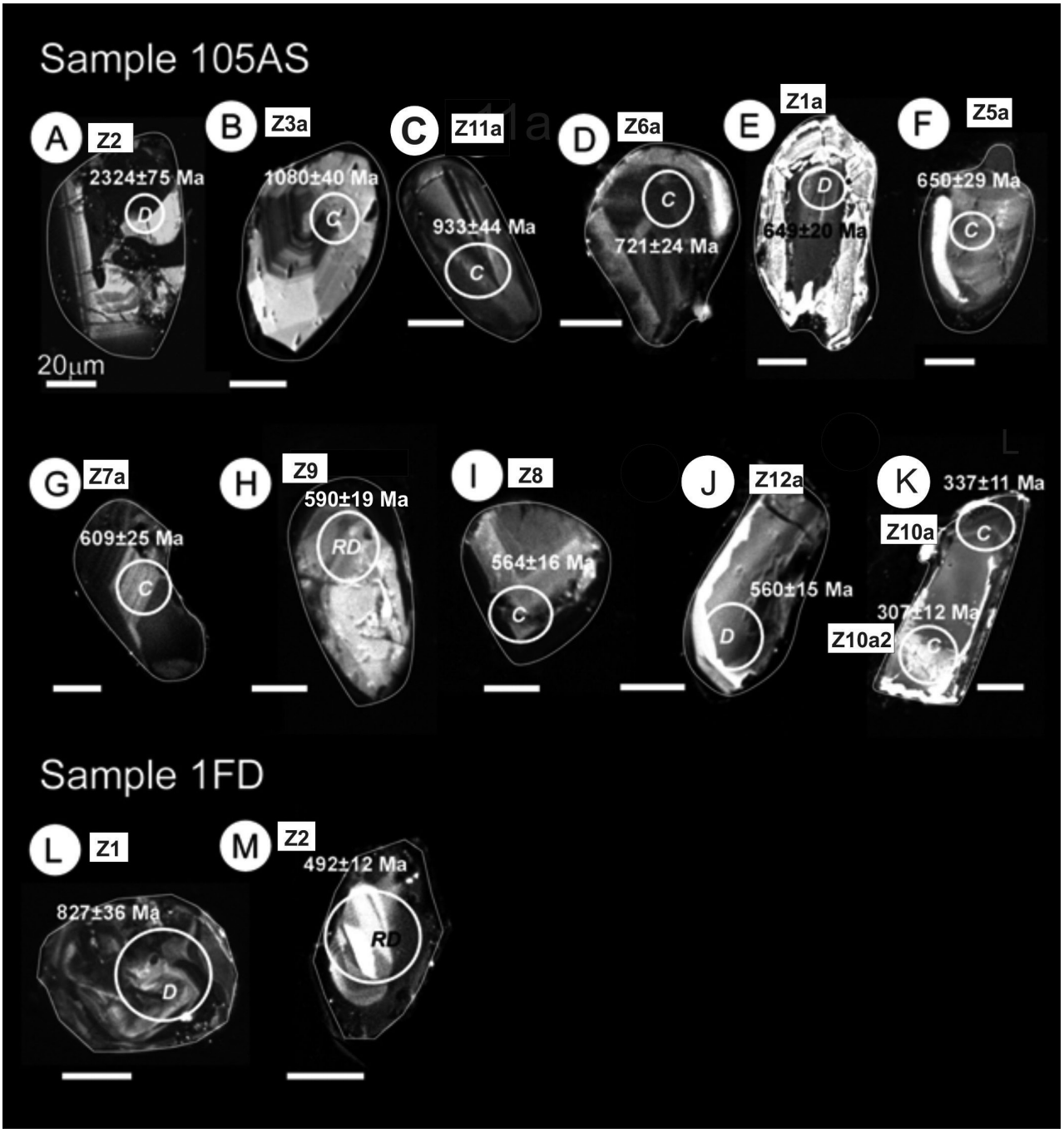

Fig. 6 - CL images of zircons in sample 105AS (panels A-K) and sample 1FD (panels L and M). C= concordant; D= discordant, and R= reversely discordant. Scale bar is 100μm. Letters for individual zircons are the same as listed in table 1.

105AS, Z9: Figs. 5F, 5G, 6M, 6H). Reverse discordance can occur either when radiogenic Pb migrates from high into low U parts of finely zoned crystals, or when metamorphic or hydrothermal fluids attack the zircon crystal and selectively mobilize U from domains that were strongly metamict (Mattinson et al., 1996).

The reverse discordant zircons of the rhyolite (sample 10FT) at the base of the section are the youngest ages in a cluster extending back to 600 Ma. Disregarding these two zircon ages, the best age for the rhyolite is the concordant Z5 with an age of 516±15 Ma (Fig. 7; Tab. 1) The chert sample 1FD gave two ages, one of which (Z1) is Neoproterozoic (827±36 Ma), the other (Z2) is one of the reversely discordant zircons with a late Cambrian age (492±12Ma). The volcaniclastic sample 105AS yields ages, apart from two discordant young ages around 300 Ma, older than 560 Ma and older than sample 10FT stratigraphically below.

5. DISCUSSION

For the Montalto Formation rhyolite zircons (sample 10FT) the youngest acceptable eruption age, omitting the reverse discordant zircon ages is 516±15 Ma (Fig. 7).

Tab. 1. Summary of zircon ages obtained in this study.

Zircon	$^{238}U/^{206}Pb$ Age (±1σ)	$^{235}U/^{207}Pb$ Age (±1σ)	$^{207}Pb/^{206}Pb$ Age (±1σ)	$\%^{206}Pb^{*}$ (±1σ)	Th+/U+ (±1σ)	Figure
Sample 10FT						
Z3 [a]	1743 (45)	1709 (42)	1668 (72)	100.0 (0.5)	0.216 (0.012)	5A
Z20	609 (21)	598 (22)	555 (82)	99.0 (0.2)	0.256 (0.003)	5B
Z1	561 (21)	559 (19)	552 (410	99.9 (<0.01)	0.312 (0.004)	5C
Z21	531 (18)	540 (15)	582 (42)	99.9 (<0.01)	0.158 (0.044)	5D
Z5	516 (15)	518 (12)	524 (38)	99.8 (<0.01)	0.352 (0.012)	5E
Z14	484 (15)	475 (15)	428 (49)	99.3 (0.1)	0.080 (0.002)	5F
Z4 [a]	454 (17)	453 (17)	450 (55)	99.7 (0.1)	0.045 (0.003)	5G
Z6 [a]	332 (13)	322 (13)	248 (63)	99.9 (0.1)	0.064 (0.001)	5H
Z19 [a]	327 (12)	326 (37)	319 (270)	100.0 (0.7)	0.370 (0.007)	5I
Z12 [a]	324 (10)	334 (9)	400 (52)	100.1 (0.1)	0.093 (0.002)	5J
Z15	318 (15)	348 (34)	551 (219)	99.4 (0.6)	0.339 (0.007)	5K
Z2	315 (19)	208 (88)	-	97.1 (1.7)	0.321 (0.014)	5L
Z11 [a]	313 (12)	312 (11)	303 (46)	99.9 (0.1)	0.041 (0.001)	5M
Z9 [a]	310 (9)	316 (8)	358 (32)	99.7 (0.1)	0.038 (<0.001)	5N
Z17 [a]	303 (10)	302 (15)	295 (109)	99.7 (0.3)	0.169 (0.005)	5O
Z8	297 (9)	298 (8)	308 (31)	99.7 (0.1)	0.026 (<0.001)	5P
Z10	151 (5)	142 (11)	-	99.2 (0.3)	0.166 (0.002)	5Q
Z13 [a]	85.9 (3.5)	87 (11)	116 (284)	99.2 (0.7)	0.339 (0.002)	5R
Sample 1FD						
Z1	827 (36)	992 (37)	1378 (37)	99.5 (0.1)	0.083 (0.002)	6L
Z2	492 (12)	463 (21)	319 (113)	98.2 (0.3)	0.380 (0.004)	6M
Sample 105AS						
Z2	2324 (75)	2388 (39)	2443 (14)	99.8 (<0.01)	0.119 (0.002)	6A
Z3a	1080 (40)	1070 (57)	1049 (160)	99.9 (0.7)	0.444 (0.010)	6B
Z11a	933 (44)	917 (36)	877 (66)	99.8 (0.3)	0.144 (0.006)	6C
Z6a	721 (24)	717 (23)	704 (61)	99.9 (0.2)	0.198 (0.003	6D
Z5a	650 (29)	657 (31)	683 (84)	100.0 (0.3)	0.292 (0.003	6F
Z1a	649 (20)	782 (88)	1184 (297)	96.4 (1.1)	0.324 (0.003)	6E
Z7a	609 (25)	625 (22)	683 (62)	100.1(0.2)	0.165 (0.002)	6G
Z9	590 (19)	527 (27)	264 (121)	98.5 (0.3)	0.065 (0.003)	6H
Z8	564 (16)	561 (18)	549 (51)	99.4 (0.1)	0.126 (0.002)	6I
Z12a	560 (15)	600 (40)	753 (167)	100.1 (0.7)	0.518 (0.008)	6J
Z10a	337 (11)	337 (10)	334 (30)	100.0 (0.1)	0.095 (0.001)	6K
Z10a2	307 (12)	305 (12)	287 (61)	99.9 ((0.1)	0.087 (0.002)	6K

[a] Zircon age calculated using ^{206}Pb correction. All other ages corrected using a ^{204}Pb correction.
Ages calculated with Isoplot (Vermeesch, 2018)

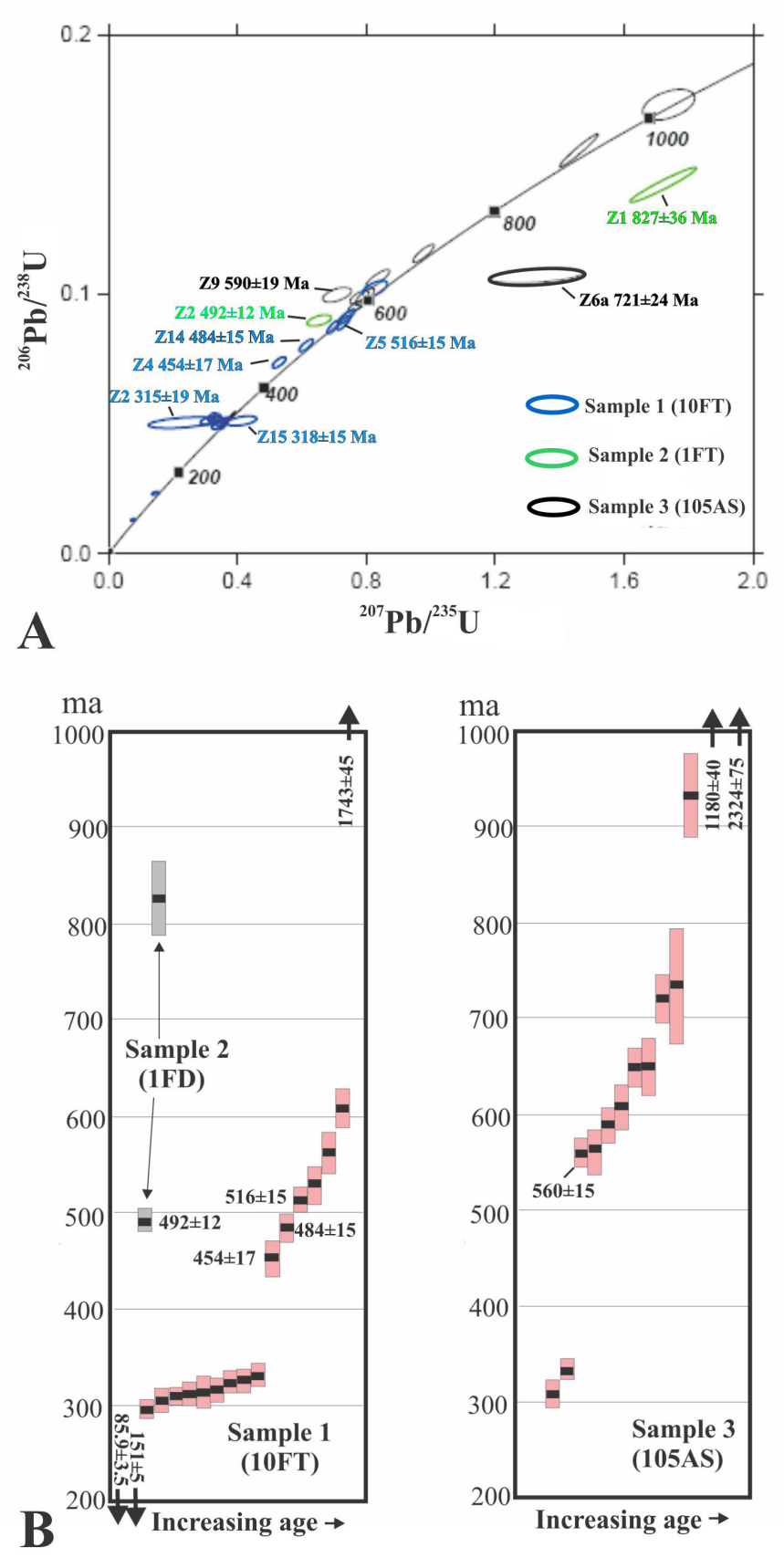

Fig. 7 - A) Conventional Concordia plot of $^{206}Pb/^{238}U$ against $^{207}Pb/^{235}U$ (Wetherill, 1956) for individual Valongo zircon analyses, using Isoplot (Ludwig, 2012). Concordia curve is the locus of points where the $^{238}U/^{206}Pb$ age equals the $^{235}U/^{207}Pb$ age; B) distribution of $^{238}U/^{206}Pb$ ages for the analyzed samples. Error bars are ±1σ.

This is Middle Cambrian (Series 2) and dates rhyolitic volcanism associated with rifting in the Valongo anticline (Couto and Roger, 2017). In the South Armorican and Occitan Variscan domains of France, similar rift valley rhyolites, give a U/Pb zircon age of 519+14/-10 Ma, which is well within the error of the Montalto rhyolite dated here (Ballèvre et al., 2012). These are separated from overlying Arenigian quartzites by very thick rhyolites of latest Cambrian to Tremadocian age (490-480 Ma), marking the main uplift, rifting and tectonic break-up of the North Gondwana margin (Pouclet et al., 2017). The thinness, or absence, of such rhyolites in the Valongo Anticline area may be due to it forming a positive rift shoulder uplift during the initial rifting and magmatic episode on the Gondwana passive continental margin accompanying the opening of Rheic Ocean (Couto, 2013; Couto et al., 2014)

The younger zircon ages of sample 10FT range from 332 to 397 Ma, are also close to concordant, and are interpreted as zircon recrystallization during Upper Carboniferous Variscan hydrothermal alteration and regrowth (Fig. 5 H-R). These Variscan ages are associated with the Sb-Au mineralization of the Valongo anticline and Douro Shear Zone (Couto, 1993; Couto and Roger, 2017), part of the extensive Sb-Au Variscan mineralization of Armorica (Pochon et al., 2018). A significant late Carboniferous–Permian Variscan tectonic episode reworked the southern European crust, causing localized magmatic recycling, extension and transcurrent faulting and the development of localized sedimentary basins (Schulmann et al., 2014). The two youngest concordant zircons (151±5; 85.9±3.5) may indicate hydrothermal alteration during rifting that accompanied the opening of the Central Atlantic Ocean and anticlockwise rotation of Iberia (Seton et al., 2012).

For the lower Santa Just Formation black chert zircons (sample 1FD), of the two zircon ages, the youngest age of 492±12 Ma (Upper Cambrian, Furongian) is reversely discordant and thus too old; although it does suggest that the basal Santa Justa Formation is post Upper Cambrian in age.

For the upper Santa Justa Formation volcaniclastic sandstone (sample $3, 105AS), the zircons are all detrital and date only the source rocks of the sediments. The youngest acceptable zircon age (560±15 Ma) is Neoproterozoic, and older than the Upper Cambrian to Middle Ordovician age of the Formation from its stratigraphic position. The entire Santa Justa Formation is thus probably Arenigian, although a Tremadocian age for its base cannot be ruled out.

The detrital zircon ages are dominantly Neoproterozoic, with only one Mesoproterozoic and one Paleoproteroic age (Fig. 7), a distribution very similar to age-equivalent metasediments in the southeastern Pyrenees. The latter, however, also has a late Archean (2.4-2.6 Ga) peak (Margalef et al., 2016). These ages fit sources along the northern edge of the reworked Neoproterozoic Saharan metacraton forming a 2300 km east-west aligned northern Gondwana passive margin (Liégeois et al., 2013; Shaw et al., 2014; Shaw and Johnson, 2016).

6. CONCLUSIONS

The rhyolite near the top of the Montalto Formation gave a youngest zircon age of 516±15 Ma (Series 2, mid-Cambrian), which is likely a reasonable age for this rapidly deposited succession of rift valley bimodal basalt/rhyolite lavas and coarse clastics. The younger zircon dates around 300 Ma are due to hydrothermal zircon crystallization during Upper Carboniferous Variscan deformation.

The black chert at the base of the Santa Justa Formation produced only two zircon ages; the youngest of which (492±12 Ma; Upper Cambrian, Furongian) is from a reversely discordant crystal and is thus too old. Thick Latest Cambrian to Tremadocian rift valley rhyolites present in Armorica and the Galician-Castilian Zone to the north and marking the main tectonic break-up of the North Gondwana margin, are thin or absent in the Valongo anticline which may have formed part of an uplifted eroding rift block at the time.

The volcaniclastic sandstone near the top of the Santa Justa Formation zircon ages are entirely from detrital zircons and give a youngest zircon date of 560±15 Ma (Neoproteroizc, Ediacaran), older than the Formation's stratigraphically constrained Upper Cambrian to Middle Ordovician. These older zircon age patterns are similar to those of equivalent metasediments in the southeastern Pyrenees, and these two areas could have shared the same Lower Ordovician source area, the northern edge of the reworked Proterozoic Saharan metacraton.

Further study of suitable zircon-bearing volcanic rocks is needed to accurately date, especially the lower unit of the Santa Justa Formation.

ACKNOWLEDGEMENTS - This is a contribution to ICT Institute of Earth Sciences, Department of Geosciences, Environment and Spatial Planning, University of Porto and to the IGCP Project 653. Funding for the geochemical analyses by E Catlos was provided by the Jackson School of Geosciences at The University of Texas at Austin. Age data were collected by E. Catlos and S. Suarez with the assistance of the Max Kade Foundation. SIMS facilities at Heidelberg University acknowledge support through DFG Scientific Instrumentation and Information Technology. We appreciate analytical assistance by Thomas Etzel and the critical revision of the manuscript by two anonymous reviewers.

REFERENCES

Ballèvre M., Fourcade S., Capdevila R., Peucat J.-J., Cocherie A., Fanning C.M., 2012. Geochronology and geochemistry of Ordovician felsic volcanism in the Southern Armorican Massif (Variscan belt, France): Implications for the breakup of Gondwana. Gondwana Research 21, 1019-1036.

Catalán J.R.M., 2011. The Central Iberian arc: implications for the Iberian Massif. Geogaceta 50, 7-10.

Couto H., 1993. As mineralizações de Sb-Au da região Dúrico-Beirã. Ph.D thesis, Porto, Faculty of Sciences, University of Porto. 2 volumes, pp. 606.

Couto H., 2013. The Ordovician of Valongo Anticline (Northern Portugal): State of Art. Geology, Exploration and Mining. SGEM 2013 Conference Proceedings, 1, 203-208.

Couto H., Knight J., 2014. The Montalto Formation, a pre- to basal Ordovician succession in the Durico-Beirã area (northern Portugal). In: Rogerio R., Pais J., Kullberg J.V., Finney S.C. (Eds.), STRATI 2013: First International Congress on Stratigraphy at the Cutting Edge of Stratigraphy, Springer, New York, 381-384.

Couto H., Moëlo Y., 2011. Lower Ordovician oolitic ironstones of Valongo Anticline (Dúrico-Beirã area, Portugal) and of Châteaubriant Anticline (Armorican Massif, France): a comparative study. 11th SGA Biennial Meeting; Let's Talk Ore Deposits, 26-29th September 2011 Antofagasta, Chile, pp. 4.

Couto H., Roger G., 2017. Palaeozoic magmatism associated with gold-antimony-tin-tungsten-lead-zinc and silver mineralization in the neighboring of Porto, Northern Portugal. IOP Conference Series. Earth and Environmental Science 95, 1-11.

Couto H., Knight J., Lourenço A., 2014. Rifting at the Cambrian - Ordovician transition in northwestern Portugal. Comunicacoes Geologicas 101, 251-254.

Couto H., Roger G., Moelo Y., 2017. Chemical characteristics of REE-bearing phosphate minerals from Dúrico-Beirão gold-antimony mining district (Northern Portugal). International Multidisciplinary Scientific GeoConference Surveying Geology and Mining Ecology Management, SGEM 17, 11, 81-88.

Gonçalves E.J. dos Santos, 2013. Hidrogeologia das areas de Valongo, de Paredes, et de Arouca, no contexto do Anticlinal de Valongo. Thesis, Univeristad de Porto, Portugal, pp. 355.

Gutiérrez-Marco J.C., Sá A.A., García-Bellido D.C., Rábano I., Valério M., 2009. Giant trilobites and trilobite clusters from the Ordovician of Portugal. Geology 37, 443-446.

Gutiérrez-Marco J.C., Sá A.A., Rábano I., Sarmiento G.N., García-Bellido D.C., Bernárdez E., Lorenzo S., Villas E., Jiménez-Sánchez A., Colmenar J., Zamora S., 2015. Iberian Ordovician and its international correlation. Stratigraphy 12, 257 -263.

Gutiérrez-Marco J.C., Sá A.A., García-Bellido D.C., Rabano I., 2017. The Bohemo-Iberian regional chronostratigraphical scale for the Ordovician System and palaeontological correlations within South Gondwana. Lethaia 50, 258 -295.

Hoke J.D., Schmitz G.D., Bowring S.A., 2014. An ultrasonic method for isolating nonclay components from clay-rich material. Geochemistry, Geophysics, Geosystems 15, 492-498.

Liégeois J.-P., Abdelsalam M.G., Ennih N., Ouabadi A., 2013. Metacraton: nature, genesis and behavior. Gondwana Research 23, 220-237.

Liñán E., Perejón A., Sdzuy K., 1993. The Lower-Middle Cambrian stages and stratotypes from the Iberian Peninsula: a revision. Geological Magazine 130, 817-833.

Linnemann U., Pereira M.F., Jeffries T., Drost K., Gerdes A., 2008. The Cadomian Orogeny and the opening of the Rheic Ocean: the diachrony of geotectonic processes constrained by LA-ICP-MS U -Pb zircon dating (Ossa-Morena and Saxo-Thuringian Zones, Iberian and Bohemian Massifs). Tectonophysics 61, 21-43.

Lotze F., 1945. Zur gliederung der Varisziden der Iberischen Meseta. Geotektonische Forschungen 6, 78-92.

Ludwig K.R., 2012. Isoplot 3.75: A geochronological toolkit for Microsoft Excel. Berkeley Geochronology Center, Special Publication 5, 1-75.

Lukács R., Guillong M., Schmitt A., Molnár K., Bachmann O., Harangi S., 2018. LA-ICP-MS and SIMS U-Pb and U-Th zircon geochronological data of Late Pleistocene lava domes of the Ciomadul Volcanic dome complex (Eastern Carpathians). Data in Brief, 18, 808-813.

Margalef A., Castiñeiras P., Casas J.M., Navidad M., Liesa M., Linnemann U., Hofmann I., Gartner A., 2016. Detrital zircons from the Ordovician rocks of the Pyrenees: geochronological constraints and provenance. Tectonophysics 681, 124-134.

Mattinson J.M., Graubard C.M., Parkinson D.L., McClelland W.C., 1996. U-Pb reverse discordance in zircons: the role of fine-scale oscillatory zoning and sub-micron transport of Pb. AGU Geophysical Monograph Series 95, 355-370.

Mohriak W.U., Leroy S., 2013. Architecture of rifted continental margins and break-up evolution: insights from the South Atlantic, North Atlantic and Red Sea -Gulf of Aden conjugate margins, In: Mohriak W.U., Danforth A., Post P.J., Brown D.E., Tari G.C., Nemčok M., Sinha S.T. (Eds.), Conjugate Divergent Margins. Geological Society, London, Special Publications 369, 497-536.

Murphy J.B., Gutiérrez-Alonso G., Nance R.D., Fernández-Suárez J., Keppie J.D., Quesada C., Strachan R.A., Dostal J., 2006. Origin of the Rheic Ocean: Rifting along a Neoproterozoic suture? Geology 34, 325 -328.

Pochon A., Gloaguen E., Branquet Y., Poujol M., Ruffet G., Boiron M-C., Boulvais P., Gumiaux C., Cagnard F., Gouazou F., Gapais D., 2018. Variscan Sb-Au mineralization in Central Brittany (France): A new metallogenic model derived from the Le Semnon district. Ore Geology Reviews 97, 109-142.

Pouclet A., Álvaro J.J., Bardintzeff J.M., Imaz A.G., Monceret E., Vizcaïno D., 2017. Cambrian -early Ordovician volcanism across the South Armorican and Occitan domains of the Variscan Belt in France: continental break-up and rifting of the northern Gondwana margin. Geo-science Frontiers 8, 25-64.

Reyes-Abril J., Villas E., Gutiérrez-Marco J.C., 2010. Orthid brachiopods from the Middle Ordovician of the Central Iberian Zone, Spain. Acta Palaeontologica Polonica 55, 285-308.

Ribeiro A., Munhá J., Dias R., Mateus A., Peirera E., Ribeiro L., Fonseca P., Araújo A., Oliveira T., Romão J., Chaminé H., Coke C., Pedro J., 2007. Geo-dynamic evolution of the SW Europe Variscides. Tectonics 26, 1-24.

Romano M., 1982. The Ordovician biostratigraphy of Portugal - a review with new data and re-appraisal. Geological Journal 17, 89-110.

Romano M., Diggens J.N., 1974. The stratigraphy and structure of Ordovician and associated rocks around Valongo, north Portugal. Comunicações dos Serviços Geológicos de

Portugal 57, 23 -50.

Sá A.A., Gutiérrez-Marco J.C., Piçarra J.M., García-Bellido D.C., Vaz N.M., Aceñolaza G.F., 2011. Ordovician vs. "Cambrian" ichnofossils in the Armorican quartzite of central Portugal. In: Gutiérrez-Marco J.C., Rábano I., García-Bellido D. (Eds.), Ordovician of the World. Cuadernos del Museo Geominero, 14. Instituto Geológico y Minero de España, Madrid. 483-492.

Schmitz M.D., Bowring S.A., Ireland T., 2003. Evaluation of Duluth Complex anorthositic series (AS3) zircon as a U-Pb geochronological standard: new high-precision isotope dilution thermal ionization mass spectrometry results. Geochimica et Cosmochimica Acta 67, 3665-3672.

Schulmann K., Martínez Catalán J.R., Lardeaux J.M., Janoušek V., Oggiano G., 2014. The Variscan orogeny: extent, timescale and the formation of the European crust. In: Schulmann K., Martínez Catalán J.R., Lardeaux J.M., Janoušek V., Oggiano G., (Eds.), The Variscan Orogeny: Extent, Timescale and the Formation of the European Crust. Geological Society, London, Special Publication 405, 1-6.

Seton M., Müller R.D., Zahirovic S., Gaina C., Torsvik T., Shephard G., Talsma A., Gurnis M., Turner M., Maus S., Chandler M., 2012. Global continental and ocean basin reconstructions since 200 Ma. Earth-Science Reviews 113, 212-270.

Shaw J., Johnson S.T., 2016. Terrane wrecks (coupled oroclines) and paleomagnetic inclination anomalies. Earth-Science Reviews 154, 191-209.

Shaw J., Gutiérrez-Alonso G., Johnston S.T., Pastor Galán D., 2014. Provenance variability along the Early Ordovician north Gondwana margin: paleogeographic and tectonic implications of U-Pb detrital zircon ages from the Armorican Quartzite of the Iberian Variscan belt. Geological Society of America Bulletin 126, 702 -719.

Soares D.M., Alves T.M., Terrinha P., 2012. The breakup sequence and associated lithospheric breakup surface: their significance in the context of rifted continental margins (West Iberia and Newfoundland margins, North Atlantic). Earth and Planetary Science Letters 401, 116-131.

Stampfli G.M., Borel G.D., 2002. A plate tectonic model for the Paleozoic and Mesozoic constrained by dynamic plate boundaries and restored synthetic oceanic isochrones. Earth and Planetary Science Letters 196, 17-33.

Vermeesch P., 2018. IsoplotR: a free and open toolbox for geochronology. Geoscience Frontiers 9, 1479-1493.

Wetherill G.W., 1956. Discordant uranium-lead ages, I. Transactions of the American Geophysical Union 37, 320-326.

Whitney D.L., Evans B.W., 2010. Abbreviations for names of rock-forming minerals. Mineralogical Magazine 95, 185-187.

Young T.P., 1992. Ooidal ironstones from Ordovician Gondwana: a review. Palaeogeography, Palaeoclimatology, Palaeoecology 99, 321-347.